PCCP

PAPER

Published on 17 October 2018
Licence and permissions

Check for updates

Cite this: *Phys. Chem. Chem. Phys.*, 2018, **20**, 26837

Nonadiabatic effects on the positions and lifetimes of the low-lying rovibrational levels of the GK $^1\Sigma_g^+$ and H $^1\Sigma_g^+$ states of H_2

Nicolas Hölsch, Maximilian Beyer† and Frédéric Merkt *

Received 16th August 2018,
Accepted 12th September 2018

DOI: 10.1039/c8cp05233f

rsc.li/pccp

The term values of rovibrational levels of the GK $^1\Sigma_g^+$ and H $^1\Sigma_g^+$ states of H_2 have been measured with absolute and relative accuracies down to 10^{-4} cm^{-1} ($\approx$3 MHz) and 10^{-6} cm^{-1} ($\approx$30 kHz), respectively, by measuring transitions to long-lived high-n Rydberg states using single-mode cw laser radiation and a collimated supersonic beam of cold H_2 molecules. The term values are compared with those determined in earlier experimental and theoretical investigations and the comparison points at discrepancies and a need for improved theoretical treatments of nonadiabatic, relativistic and radiative corrections for these states. The lifetimes of several low-lying rovibrational levels of the GK, H and I^+ $^1\Pi_g$ states have been determined in pump–probe experiments. These lifetimes reveal a significant dependence on the electronic, vibrational and rotational excitation and also deviate from results obtained in earlier experimental and theoretical investigations.

1 Introduction

Recent progress in *ab initio* calculations of the properties of one- and two-electron molecules makes them attractive for comparison with precision spectroscopic data.[1–5] Although the lowest rovibrational levels of the electronic ground state of the molecular hydrogen ion can be calculated with an uncertainty dominated by the uncertainty of the fundamental constants,[1] this level of accuracy has not been reached yet for the highest rovibrational states of H_2^+ nor for any of the rovibronic states of the neutral hydrogen molecule. Complications in the numerical calculation of rovibronic energies originate from nonadiabatic effects, which scale with the inverse of the reduced mass, and are thus particularly strong in light systems. Nonadiabatic effects arise because of the entangled motion of the electrons and the nuclei. They appear as off-diagonal terms (*i.e.*, connecting different electronic states) in the molecular Hamiltonian derived in a Born–Oppenheimer framework. The resulting rovibronic interactions lead to small energy shifts of the lowest rovibrational levels of the electronic ground states in H_2 and H_2^+ because interacting electronically excited states are energetically very distant. Rovibrational levels in the vicinity of the first dissociation thresholds H(1s) + H(1s) and H(1s) + H^+ are also affected by nonadiabatic interactions resulting from the hyperfine Hamiltonian[6,7] and the associated g/u-symmetry breaking.

Rovibronic nonrelativistic level energies in H_2^+ and H_2 (and the deuterated and tritiated isotopomers) are calculated using either (i) nonadiabatic perturbation theory within the framework of the Born–Oppenheimer approximation[8,9] or (ii) pre-Born–Oppenheimer techniques,[1,10–12] which involve the direct solution of the three- and four-body Schrödinger equations. In the case of H_2^+, an accuracy of better than 3 kHz was obtained for the lowest rovibrational levels of the electronic ground state.[1] When comparing the nonrelativistic energies with the results of calculations in the adiabatic approximation (*i.e.*, ignoring all off-diagonal terms in the Hamiltonian), the nonadiabatic corrections are found to be less than 0.5 cm^{-1} in the ground rovibronic state of both H_2 and H_2^+.[13]

To reach the accuracy of the best experimental measurements, the leading-order relativistic ($\mathcal{R}\alpha^2$) and QED ($\mathcal{R}\alpha^3$) corrections and higher-order QED corrections have to be included. Until recently, these corrections were calculated for H_2 by using electronic Born–Oppenheimer wave functions, which resulted in a small but significant disagreement between the theoretical and experimental dissociation energies of the hydrogen molecule.[2,5] In recent works,[3,14] the nonadiabatic contribution to the relativistic correction to the dissociation energy of H_2 has been determined to be of the order of 60 MHz, which corresponds to roughly 1% of the $\mathcal{R}\alpha^3$ term but is slightly larger than the $\mathcal{R}\alpha^4$ correction. The nonadiabatic contributions to the QED corrections are unknown in the case of the electronic ground state of H_2.

Laboratory of Physical Chemistry, ETH Zurich, CH-8093 Zurich, Switzerland. E-mail: frederic.merkt@phys.chem.ethz.ch

† Present address: Sloane Physics Laboratory, Yale University, 217 Prospect St, New Haven CT 06511, USA.

In contrast to the ground state, electronically excited states are more strongly affected by nonadiabatic effects because of the higher state density. Consequently, the calculations of relativistic and QED corrections in these states are particularly challenging. The best nonadiabatic calculations for the lowest excited states of H_2 were carried out by Quadrelli, Dressler and Wolniewicz[15] and reached an accuracy of about 1 cm^{-1} for the GK $^1\Sigma_g^+$ and H$\bar{H}$ $^1\Sigma_g^+$ states. The leading-order relativistic corrections for these states were calculated using electronic Born–Oppenheimer wave functions, and the leading-order radiative corrections were not calculated but were taken equal to the values obtained for H_2^+.[16]

So far, only very fragmentary high-accuracy spectroscopic data are available on the electronically excited states of these molecules. In the case of H_2, Altmann *et al.*[17] have measured the intervals between the X $^1\Sigma_g^+(v = 0, N = 1)$ ground state and the EF $^1\Sigma_g^+(v = 0, N = 1)$ excited state at an accuracy of 73 kHz ($\Delta\nu/\nu = 2.4 \times 10^{-11}$). Beyer *et al.*[18] have reported the interval between the GK $^1\Sigma_g^+(v = 0, N = 2)$ and high Rydberg states at an accuracy of 64 kHz ($\Delta\nu/\nu = 1.7 \times 10^{-10}$).‡

In this article, we report on a measurement of the rovibronic energies of several levels of the double-minimum GK $^1\Sigma_g^+$ state and of the inner well (H) of the H$\bar{H}$ $^1\Sigma_g^+$ state with unprecedented relative and absolute accuracies down to 30 kHz and 3 MHz, respectively. The double-minimum GK state results from the avoided crossings of the potential curves of the $(1s\sigma_g3d\sigma_g)$, $(2p\sigma_u)^2$ and $(1s\sigma_g2s\sigma_g)$ configurations, whereas the H state corresponds to the $(1s\sigma_g3s\sigma_g)$ configuration. Both of these states are almost degenerate with the I $^1\Pi_g$ state, which is of the dominant $(1s\sigma_g3d\pi_g)$ configuration. The degeneracy of the potential curves belonging to the 3d complex and the s–d interaction leads to nonadiabatic level shifts of the order of 200 cm^{-1}, as large as the adiabatic corrections. The theoretical description of these states poses more stringent requirements on the calculations of nonadiabatic, relativistic and QED effects than the electronic ground state or the EF state of the hydrogen molecule, which are energetically "isolated". The first goal pursued in the investigations presented in this article was to provide a reliable set of rovibronic energies for the GK and H states of H_2.

We also report on measurements of the lifetimes of the rovibrational levels of the GK and H states, which lead to a line broadening in high-resolution spectra of transitions to long-lived Rydberg states. The lifetimes were determined using a pump–probe excitation scheme and were independently validated by the analysis of lineshapes observed in the frequency-resolved measurements. The lifetimes of the GK and H states are known to be primarily limited by radiative decay with a smaller contribution from predissociation.[19] Both decay mechanisms are expected to also reflect nonadiabatic effects, but no full theoretical treatments have been reported so far. Recently, Astashkevich and Lavrov[20] have presented a detailed review of the current knowledge on the lifetimes of excited states of molecular hydrogen and pointed at numerous deficiencies and the need for additional experimental studies. Our second goal was to contribute to filling this gap.

‡ Because only singlet low-lying electronic states are considered in this work, we use the quantum number N of the total angular momentum without spin to label the rotational states instead of the quantum number J of the total angular momentum without nuclear spin.

2 Experimental procedure

The laser system and vacuum chambers used in the present work have been described in ref. 18, to which we refer for details. The experiments are carried out using H_2 molecules in pulsed doubly-skimmed supersonic expansions produced by a cryogenically cooled (T = 50 K) valve designed to generate short pulses (typical duration 50 μs). Under these conditions, only the lowest levels of para (N'' = 0) and ortho (N'' = 1) H_2 are populated in the ground X $^1\Sigma_g^+$ state. To access and detect the GK (v = 0–2, N = 0–3) and the H (0, N = 0–3) states, we use the resonant three-photon excitation schemes

$$\begin{aligned} \mathrm{X}\ {}^1\Sigma_g^+(0, N'' = 0, 1) &\xrightarrow{\mathrm{VUV}} \mathrm{B}\ {}^1\Sigma_u^+(4, N' = 1, 2) \\ &\xrightarrow{\mathrm{VIS}} \mathrm{GK\ or\ H}\ {}^1\Sigma_g^+(v, N) \\ &\xrightarrow{\mathrm{NIR}} n/\varepsilon l N_{N^+}(v^+)[\mathrm{H_2}^+\ \mathrm{X}^+], \end{aligned} \tag{1}$$

as depicted schematically in Fig. 1. Starting from the ground-state level with N'' = 0 (N'' = 1), gerade electronically excited states with N = 0, 2 (N = 1, 3) can be reached. To drive the B ← X transition, pulsed vacuum-ultraviolet (VUV) laser radiation (pulse length ~3 ns, pulse energy ~1 nJ) generated by resonance-enhanced four-wave mixing in xenon (see ref. 18) was used. The visible (VIS) laser used to excite to the double-well states from the B state is a commercial Nd:YAG-pumped dye laser (pulse duration 8 ns, bandwidth 0.03 cm^{-1}), attenuated to about 1 μJ per pulse to avoid resonance-enhanced multiphoton ionisation.

To determine the positions of the rovibrational levels of the GK and H states, we record the transitions to long-lived high-np and f Rydberg states belonging to a series converging on the $X^+(v^+ = 0–1, N^+ = 0–3)$ levels of H_2^+ with a single-mode (bandwidth <100 kHz) continuous-wave near-infrared (NIR) laser stabilised and calibrated using a frequency comb (calibration accuracy better than 3 kHz). The relative positions of the double-well states and their uncertainties are determined by recording a redundant network of transitions and extracting combination differences in a weighted least-squares fit with weights derived from the uncertainties of the individual measurements. The absolute term values are derived from the relative positions using intervals reported in ref. 5 and 22–25 (see Section 3.1).

To determine the lifetimes of the rovibrational levels of the GK, H and I^+ states, we use a pulsed NIR laser, pumped by a second Nd:YAG laser, to excite high Rydberg states ($n > 50$) and subsequently field-ionise them and monitor the H_2^+ ion signal as a function of the delay between the visible (pump) and NIR (probe) laser pulses. The transitions to the high Rydberg states were far from saturated. Fig. 2 illustrates the measurement procedure with the example of the GK(2,1) state accessed *via* the B(4,2) state. The black dots in the top panel (a) correspond to the normalised integrated ion signals measured as a

 This journal is © the Owner Societies 2018

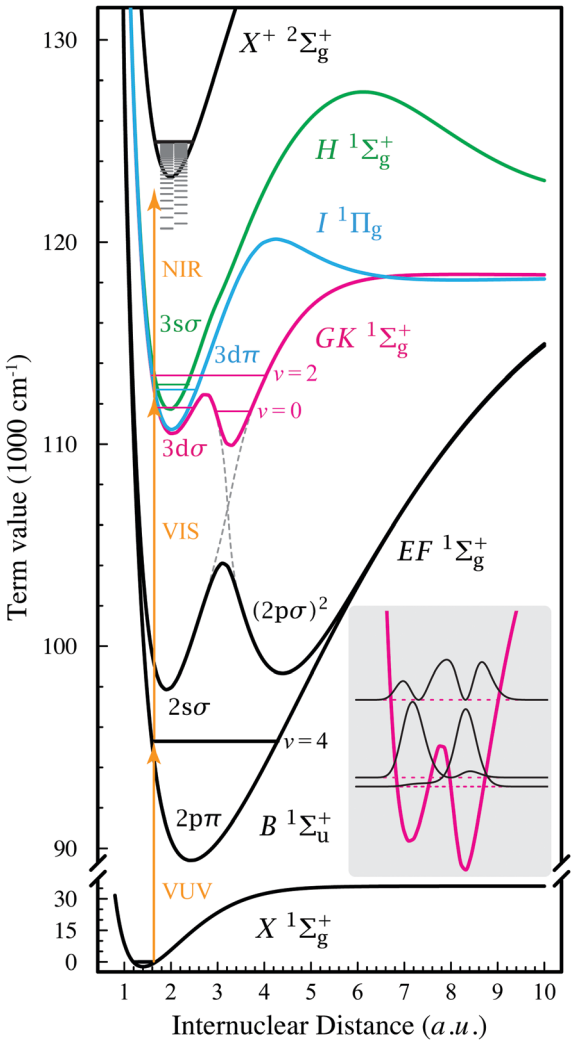


Fig. 1 Potential energy functions and dominant electron configurations of the electronic states of H_2 relevant for the present investigation, taken from ref. 21. The notation implies that the core electron is in the ($1s\sigma_g$) orbital when only one orbital is specified. The horizontal bars indicate the positions of the vibrational levels, and the inset depicts the corresponding squared wavefunctions for the GK $^1\Sigma_g^+(v = 0–2)$ levels. The multiphoton excitation scheme is indicated by vertical arrows.

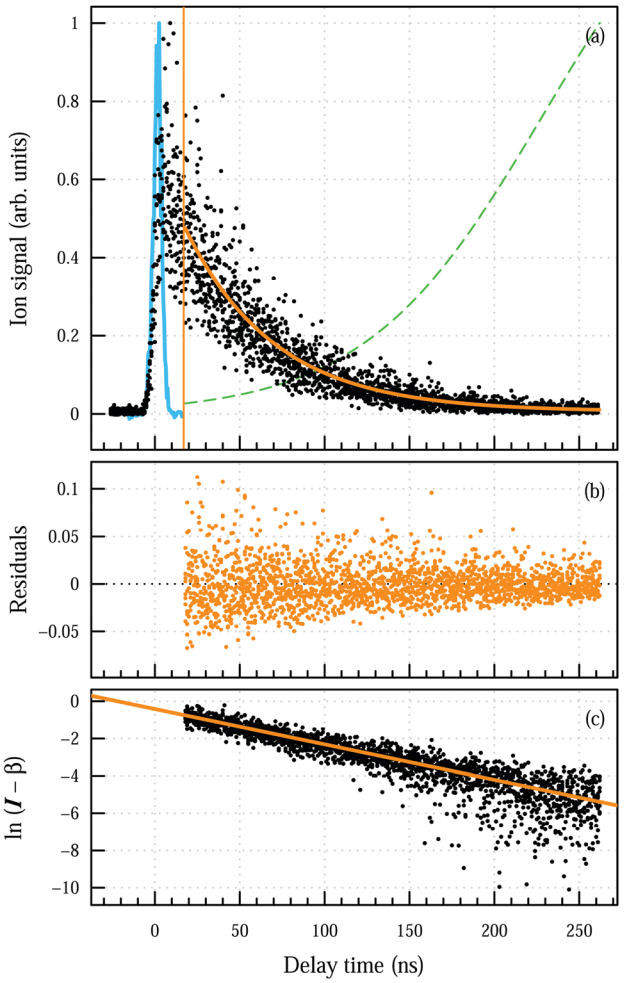


Fig. 2 (a) Normalised ion signal for the pump–probe lifetime measurement of the GK(2,1) state (black dots). The blue trace is the ion signal obtained upon ionizing the B(4,2) intermediate state without turning on the GK(2,1) ← B(4,2) excitation laser and represents the instrument function. The solid orange line corresponds to a weighted fit of eqn (2) to the experimental data, and the vertical line marks the earliest data points used in the analysis. The weights used in this fit are plotted normalised to their maximum values as a green dashed line. (b) Weighted residuals from the fit. (c) Data and fit from (a) displayed on a logarithmic scale.

function of the pump–probe delay time. The light blue line represents the ion signal generated without exciting the GK(2,1) state, but instead using a UV pulse to ionise the B(4,2) state, and thus gives the temporal resolution of the experiment (FWHM ~ 7 ns). Data points in the first 25 ns after the onset of the signal were not used to extract lifetimes in order to avoid times at which the pump and probe pulses overlap. The delay time t_0 marking the start of the analysis is indicated in Fig. 2(a) by a solid vertical line. The orange curve was obtained from a weighted fit of the truncated experimental data to the function

$$I(t) = \alpha \cdot e^{-k(t-t_0)} + \beta, \qquad (2)$$

where β is the background signal. The iterative fit procedure and the determination of the weights followed the method outlined in ref. 26.

Fig. 2(b) presents the residuals obtained in a weighted fit. A fit was considered satisfactory when the weighted residuals did not show a dependence on the delay time and were found to be normally distributed with a reduced chi-squared value close to 1. After subtracting the fitted background signal β from the data, the points were plotted together with the fitted decay curve on a logarithmic scale, as depicted in Fig. 2(c), to verify the single-exponential nature of the decay.

3 Results

3.1 Positions

In order to determine accurate relative and absolute positions of the rovibrational levels of the GK and H states, they were linked by recording transitions to a set of high-n Rydberg states,

each Rydberg state being accessed from at least two different initial levels. Rydberg states with total angular momentum (without spins) quantum numbers $N = 1$ and $N = 2$ were selected in para and ortho H_2, respectively, to observe strong transitions from $N = 0$, 2 and $N = 1$, 3 levels of the intermediate GK and H states. Most of the selected Rydberg states have principal quantum numbers n in the range between 18 and 56 in order to reduce systematic uncertainties and avoid broadening of the lineshape related to the effect of magnetic and electric stray fields (see ref. 18 for a complete discussion of systematic and statistical uncertainties), which are enhanced in high-n Rydberg states.

Examples of transitions recorded in para and ortho H_2 are depicted in Fig. 3 and 4, respectively. Each of these spectra consists of two Doppler components arising from a non-perpendicular arrangement of the propagation axes of the supersonic molecular beam and the two counter-propagating laser beams, as discussed in detail in ref. 18. Both Doppler components have a Lorentzian lineshape with an equal linewidth, which was determined together with the two centre frequencies by adjusting a sum of two Lorentzians in a non-linear regression. The Doppler-free transition frequency ν_0 is determined as the average of the centre frequencies of the two Doppler components. Energy differences are obtained from the transition frequencies by subtracting the photon recoil shift, which is of the order of 160 kHz.[18] The second-order Doppler shift is negligible in the present case.

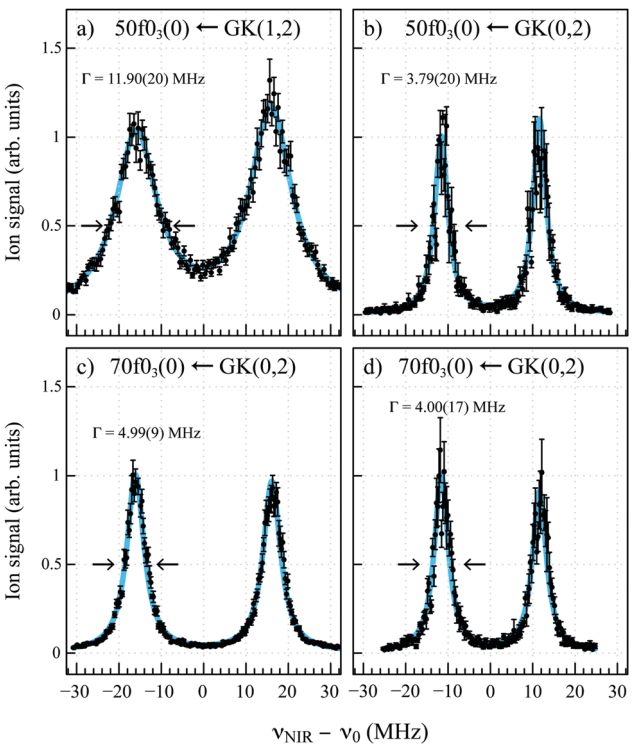


Fig. 3 Spectra of the 50f0$_3$(0) and 70f0$_3$(0) Rydberg states of H_2 recorded from the initial states GK(1,2) (panel (a)) and GK(0,2) (panels (b)–(d)). The measurements depicted on each side correspond to different experimental conditions (see text). The dots with error bars represent the experimental data and the solid blue lines the spectra determined from a fit of two Lorentzians to the data (see text for details).

The Rydberg states studied here were found to have lifetimes of more than 1 μs by delaying the pulsed-field ionisation. The lifetime broadening of the spectral lines can therefore be solely attributed to the selected rovibrational levels of the GK and H states. As an illustration, Fig. 3 displays in panels (a) and (b) the lineshapes of the 50f0$_3$(0) ← GK(1,2) and 50f0$_3$(0) ← GK(0,2) transitions, from which one immediately recognises that the lifetime of the GK(1,2) state is shorter than that of the GK(0,2) state. All observed line shapes could be fitted perfectly with Lorentzian profiles. However, we observed that the Lorentzian widths also depended weakly on the experimental conditions (primarily the operating conditions of the pulsed valve), indicating an experimental broadening mechanism not related to the natural lifetime. To quantify this broadening, we recorded the 70f0$_3$(0) ← GK(0,2) transition as a reference after each modification of the experimental conditions. The reference lines corresponding to the two spectra shown in panels (a) and (b) of Fig. 3 are plotted in panels (c) and (d), respectively. The results of the quantitative analysis of the linewidths of these four recorded transitions are presented and compared with the results of the pump–probe measurements in the next section.

In ortho H_2, the hyperfine structure of the high-n Rydberg states leads to broader spectral features because several hyperfine components are excited but are in general not resolved because of the limited lifetime of the GK and H intermediate states. However, they need to be included explicitly in the lineshape model used to extract transition frequencies. Panels (a) and (b) of Fig. 4 illustrate our measurements with the examples of the transitions from the GK(1,1) and the H(0,1) levels to the 56p1$_1$(0) Rydberg state. The former spectrum was recently used in a determination of the dissociation energy of ortho H_2.[5] In the determination of the central transition frequency, the known relative positions of the $F = 0$–2 hyperfine components (F is the total angular momentum quantum number) of the 56p1$_1$(0) state[27] were used and a statistical $(2F + 1)$ intensity distribution (see orange stick spectra) was assumed, which implies the independence of the transition probabilities of the nuclear spin. A systematic uncertainty of 200 kHz was estimated from this assumption in ref. 5. The longer lifetime of the H(0,1) state enabled a better resolution of the hyperfine structure, which in turn permitted us to validate the assumed intensity distribution and reduce the corresponding uncertainties in the hyperfine-free transition frequency and in the Lorentzian widths. The systematic uncertainty of 220 kHz of the 56p1$_1$(0) ← GK(1,1) transition reported in ref. 5 must therefore be reduced to 100 kHz.

The measured transition frequencies to the Rydberg states were combined in two networks of combination differences for transitions in para H_2 (even N values in $^1\Sigma_g^+$ states) and ortho H_2 (odd N values in $^1\Sigma_g^+$ states). In para (ortho) H_2, a total of 348 (105) transitions were measured involving 32 (22) links between 8 (8) rovibrational levels of the double-well states with 12 (8) Rydberg states. The relative positions of the rovibrational levels of the GK and H states resulting from these combination

 This journal is © the Owner Societies 2018

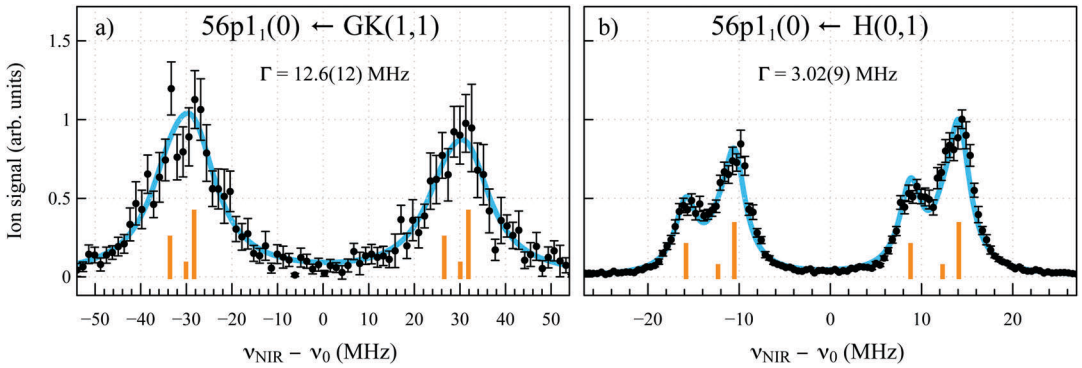


Fig. 4 Spectra of the 56p1$_1$(0) Rydberg state recorded from the initial states: (a) GK(1,1) and (b) H(0,1). The dots with error bars represent the experimental data and the solid blue lines the fit of a Lorentzian lineshape model to the data, including the hyperfine structure (see text for details). The positions and relative intensities of the hyperfine components are indicated as vertical bars.

differences are listed in the second and third columns of Table 1. Their uncertainties range from 35 kHz to 180 kHz in para H_2 and from 400 kHz to 900 kHz in ortho H_2 and reflect (i) the number of times transitions including a specific level were recorded, (ii) the number of links involving this level in the set of combination differences, (iii) the corresponding natural linewidth (lifetime) of the levels involved, broader lines yielding larger uncertainties for similar signal-to-noise ratios, and (iv) the generally unresolved hyperfine structure in ortho H_2.

Absolute term values are given in the fourth column of Table 1 and were obtained by referencing the relative energies from each combination difference to a rovibrational level with a well-known term value.

In ortho H_2, the GK(1,1) level was chosen as a reference because its position with respect to the ground state of ortho H_2 is known very precisely from Doppler-free two-photon spectroscopy.[5] The energy difference $F_0^X(1)$ = 118.48684(10) cm^{-1} between the (v = 0, N = 0) and (v = 0, N = 1) rovibrational levels of the X $^1\Sigma_g^+$ electronic ground state was taken from ref. 22 to obtain absolute level energies relative to the ground state of para H_2 (third column of Table 1). The uncertainty of the term value of the GK(1,1) level of 1.0 × 10^{-4} cm^{-1} is given by the uncertainty in the value of $F_0^X(1)$, which limits the precision of the absolute term values of all rovibrational states in ortho H_2.

In para H_2 we referenced the combination differences to the position of the GK(0,2) level because this level was the one best defined by our data set. The term value of this level, $T_{GK(0,2)}$ = 111693.73376(11) cm^{-1}, was determined with the help of the ionisation energy of ortho H_2 as

$$T_{GK(0,2)} = F_0^X(1) + E_I^{N=1}(H_2) - F_0^{X^+}(1) - E_{bind,GK(0,2)}, \quad (3)$$

using $E_I^{N=1}(H_2)$ = 124357.238062(25) cm^{-1} from ref. 5, $F_0^X(1)$ from ref. 22, $F_0^{X^+}(1)$ = 58.2336751(1) cm^{-1} from ref. 23–25 and $E_{bind,GK(0,2)}$ = 12723.757471(34) cm^{-1} from the MQDT extrapolation of measured transitions to high-n Rydberg states belonging to a series converging on the $X^+\ ^2\Sigma_g^+(0,0)$ level in H_2^+[30] (see also ref. 31). The dominant contribution to the overall uncertainty of 1.1 × 10^{-4} cm^{-1} for the GK(0,2) level is again the uncertainty

Table 1 Relative positions and absolute term values of the low-lying rovibrational levels of the GK and H electronically excited states of H_2. Δ_1 and Δ_2 give the differences of the absolute term values determined in the present work from the ones measured by Bailly *et al.*[28] and from the values calculated by Yu and Dressler,[29] respectively. All data are given in cm^{-1}

	Term values				
State(v,N)	Relative (ortho)	Relative (para)	Absolute	Δ_1	Δ_2
GK(0,0)		−64.8824237(11)	111628.85133(11)	0.040(5)	−3.34
GK(0,1)	−154.832848(13)		111650.28683(10)	0.0013(10)	−3.50
GK(0,2)		0	111693.73376(11)	0.0054(10)	−3.91
GK(0,3)	−45.178651(14)		111759.94103(10)	−0.0001(10)	−4.80
GK(1,0)		118.899781(5)	111812.63354(11)	0.005(4)	−2.667
GK(1,1)	0		111805.11968(10)	0.0096(10)	−2.850
GK(1,2)		134.0083485(22)	111827.74210(11)	0.0083(10)	−3.196
GK(1,3)	87.96524(3)		111893.08492(11)	0.0061(8)	−3.275
GK(2,0)		1699.744006(6)	113393.47776(11)	0.038(6)	−1.76
GK(2,1)	1613.742167(14)		113418.86184(10)	0.0048(20)	−2.02
GK(2,2)		1776.8377361(17)	113470.57149(11)	0.011(3)	−2.52
GK(2,3)	1745.23324(10)		113550.35292(14)	−0.0061(20)	−3.23
H(0,0)		1263.8331770(18)	112957.56693(11)	0.0071(10)	−0.89
H(0,1)	1211.627405(12)		113016.74708(10)	0.0048(6)	−1.08
H(0,2)		1440.342008(3)	113134.07576(11)	0.0088(20)	−1.58
H(0,3)	1498.326563(13)		113303.44624(10)	0.0059(8)	−3.29

in $F_0^X(1)$, indicating a need for a precise experimental link for the ortho and para level structures in H_2.

3.2 Lifetimes

Precise knowledge of the lifetimes of the rovibrational levels of the GK and H states is of fundamental interest not only from a theoretical point of view but also for the planning of high-precision spectroscopic experiments, because the lifetimes of these intermediate states limit the precision of transition frequencies to high Rydberg states, as discussed in the previous section.

Pump–probe measurements of the lifetimes of the GK(1,0) and H(0,1) states are depicted as black dots in Fig. 5 and illustrate the range of lifetimes that could be studied in the present work. In each case, the results of the unweighted and weighted fits (upper panel), and their residuals (lower panel) are plotted in light blue and orange, respectively. The results of both fits agree within their uncertainties, and the fitted curves are not distinguishable on the scale of the figure. However, the uncertainties of the fitted lifetimes are twice smaller in the case of the weighted fit. Moreover, the weighted residuals have a strongly reduced delay-time dependence. The normalised weights are indicated by the dashed green curves in the top panels and take into account the Poissonian nature of the counting process and the constant background noise of the acquisition electronics,[26] which overall results in larger weights at longer delay times when the signal is smaller.

Table 2 summarises all lifetimes measured in this work and contains data on the N = 0–3 levels of the first three vibrational levels of the GK state and the ground vibrational level of the H state, and of the N = 2 and N = 4 levels of the I^+ ground vibrational state. These lifetimes follow the overall trends reported in ref. 20 qualitatively but individual lifetimes can differ by up to 30%, the lifetimes measured in the present work being systematically shorter than those recommended in ref. 20.

Independent information on the lifetimes of the GK and H rovibrational levels can be obtained from an analysis of the linewidths of the transitions connecting these levels to long-lived Rydberg states. As an illustration, we refer to the transitions shown in Fig. 3, which were discussed briefly in the previous section. The lifetime of 58.0(7) ns measured for the GK(0,2) level in the pump–probe experiments corresponds to a full width at half maximum of 2.74(3) MHz, from which we infer that the additional experimental broadening of the reference lines in panels (c) and (d) is 2.25(12) MHz and 1.26(20) MHz, respectively. By subtracting the first value from the width obtained in panel (a), we infer that the natural linewidth of the GK(1,2) state is 9.65(32) MHz and that the corresponding lifetime is 16.5(6) ns, which we consider to be in satisfactory agreement (1.5 times the combined uncertainty) with the lifetime of 18.0(4) ns obtained in the pump–probe measurement. Repeating this procedure for other levels led to a similar level of agreement.

4 Discussion

4.1 Positions

The relative level positions of the lowest rovibrational levels of the GK and H states in ortho and para H_2 given in Table 1

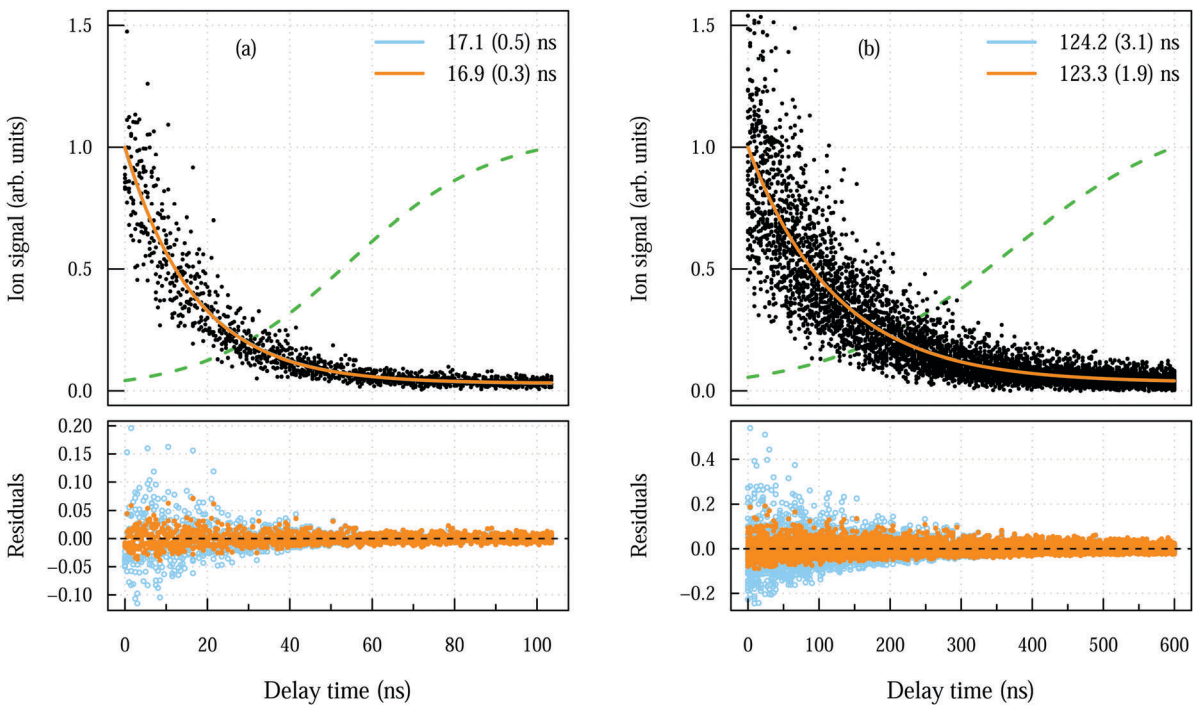


Fig. 5 Lifetime measurements of the (a) GK(1,0) and (b) H(0,1) states. The upper panels display the ionisation signal as a function of the delay between the pump and probe laser pulses. Unweighted and weighted nonlinear fits are drawn as blue and orange solid lines, respectively, but are not distinguishable by eye. The normalised weights are plotted as dashed green lines and the resulting lifetimes are indicated in the top right corners. The corresponding residuals are depicted using the same colour code in the lower panels.

This journal is © the Owner Societies 2018

Table 2 Measured lifetimes of the low-lying rovibrational levels of the GK, H and I^+ rovibrational states. The experimental lifetimes presented in the third column are the values recommended by Astashkevich and Lavrov[20] based on a compilation and evaluation of literature values published before 2015. The most important original references forming the basis for each recommendation are given in the footnotes. The lifetimes from two different theoretical approaches are given in the fourth column

	τ (ns)		
State(v,N)	This work	Experiment	Theory
GK(0,0)	78.9(17)		90.5[d]
GK(0,1)	67.2(16)	74(4)[a,b]	77.2[d]
GK(0,2)	58.0(7)	69(6)[a,b]	79.9[b]
GK(0,3)	60.6(15)	60(4)[b]	82.0[b]
GK(1,0)	16.9(3)		20.5[d]
GK(1,1)	16.9(5)	24(3)[a,c]	20.7[d]
GK(1,2)	18.0(4)	24.4(15)[a,c]	
GK(1,3)	18.6(4)	25.0(13)[c]	
GK(2,0)	66.5(28)		103[d]
GK(2,1)	52.7(10)	87(5)[a,b]	110[d]
GK(2,2)	58.1(16)	69(5)[a,b]	96.7[b]
GK(2,3)	48.2(10)	66(4)[a,b]	83.5[b]
H(0,0)	126.0(27)		102[d]
H(0,1)	123.3(19)	143(6)[b]	105[d]
H(0,2)	116.3(24)	122(5)[b]	
H(0,3)	88.4(25)	102(8)[b]	
I^+(0,2)	14.9(4)	21(2)[b,c]	16.4[b]
I^+(0,4)	17.1(2)	21.8(19)[b]	19.0[b]

[a] Ref. 32. [b] Ref. 33. [c] Ref. 34. [d] Ref. 15.

represent the most accurate measurement of the rovibronic structure of electronically excited states in molecular hydrogen. The uncertainties of the derived absolute term values are limited by the uncertainty in the value of $F_0^X(1)$, as highlighted in the previous section. Compared to the extensive survey of Bailly *et al.*,[28] the uncertainties in the positions of the states studied in this work were improved by at least a factor of 10. The term values determined in the present work are typically larger than those reported by Bailly *et al.*, and the discrepancies with the term values of Bailly *et al.* can be as large as 10 times the combined experimental uncertainties.

The experimental term values are systematically smaller than the values obtained by Yu and Dressler in a close-coupling calculation of the rovibronic structure involving nine excited electronic states of singlet gerade symmetry,[29] which have rovibrational levels below the H(1s) + H(2l) dissociation limit (see sixth column of Table 1). The differences between the observed and calculated term values are plotted in panel (c) of Fig. 6.

To relate the observed deviations to the values of the adiabatic and nonadiabatic energy corrections of the individual levels, we repeated the calculations described by Yu and Dressler[29] using the Born–Oppenheimer and adiabatic potential curves given in their work, respectively. The adiabatic and nonadiabatic corrections to the rovibronic term values as a function of $N(=J)$ are depicted in Fig. 6(a) and (b), respectively. The adiabatic corrections are independent of N, as expected. They are larger for the GK state than for the H state, reflecting the large change in the electronic character of the GK state at the avoided crossing which leads to the double-minimum structure. The $v = 0$, 2 levels of the GK state possess a larger adiabatic correction than the $v = 1$ levels, which can be related to the fact that the nuclear wave function has a larger amplitude for $R > 2.8\ a_0$ (see Fig. 1 and inset). This R-range corresponds to the region of the avoided crossings between the $(1s\sigma_g 3d\sigma_g)$, $(2p\sigma_u)^2$ and $(1s\sigma_g 2s\sigma_g)$ configurations. The nonadiabatic corrections of the GK(v = 0, 2) states (Fig. 6(b)) are positive and only weakly N-dependent, indicating a dominant homogeneous interaction (*i.e.*, $\Delta\Lambda = 0$) with the lower-lying EF state. The nonadiabatic correction of the GK(v = 1) outer-well state is almost zero for $N = 0$ but rapidly become large and negative with increasing N value. This behaviour indicates a heterogeneous perturbation (*i.e.*, $\Delta\Lambda = 1$) with the higher-lying $I\ ^1\Pi_g^+$ state (see Fig. 1). The $v = 0$ levels of the H state are only weakly perturbed because the nonadiabatic coupling elements are small for $R < 2.4\ a_0$, which corresponds to the allowed region of the H potential (see Fig. 1 and Fig. 1 of ref. 29).

The deviations between the nonadiabatic and experimental term values ($\sim -2.5\ cm^{-1}$, see Fig. 6(c)) are almost two orders of magnitude smaller than the corrections themselves, indicating the quality of the calculations of Yu and Dressler.[29] R-dependent relativistic corrections of the GK and H states were found to be of the order of $-1.5\ cm^{-1}$ by using Born–Oppenheimer electronic wave functions,[16] although the nonadiabatic contribution to the

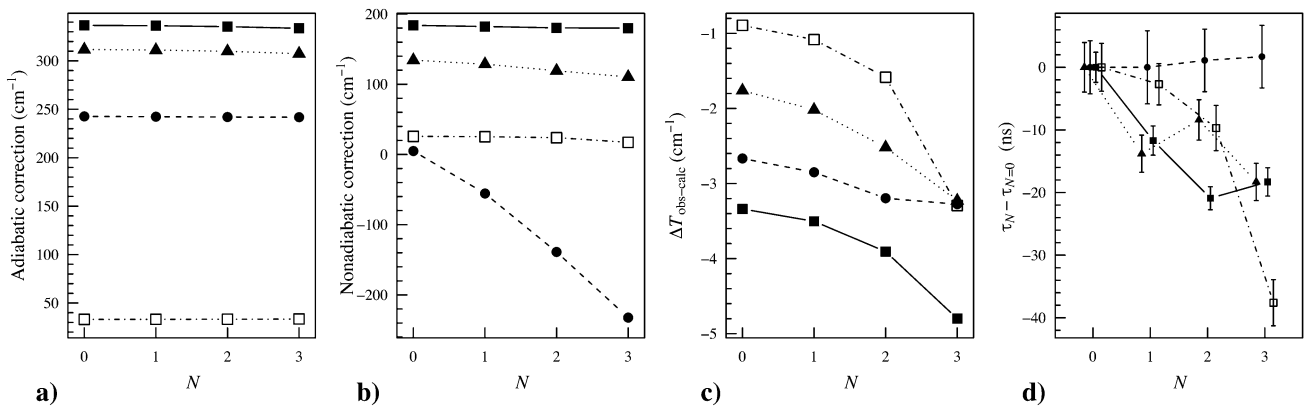


Fig. 6 Adiabatic (a) and nonadiabatic (b) corrections for the rovibronic term values of the GK and H states: ($GK(v=0) \triangleq \blacksquare$, $GK(v=0) \triangleq \bullet$, $GK(v=0) \triangleq \blacktriangle$, and $H(v=0) \triangleq \square$). (c) Deviations from the calculated term values taken from ref. 29. (d) Observed lifetimes reported in the present work relative to the lifetime of the ground rotational level of the respective vibronic state.

relativistic correction is unknown. Taking into account the relativistic correction of the X(0,0) level (~ -2.4 cm^{-1}), one can estimate that the relativistic corrections of the GK and H term values with respect to the X(0,0) ground state are about -0.9 cm^{-1} ($= -2.4$ cm$^{-1} + 1.5$ cm^{-1}). The radiative corrections are also unknown for these states but can be approximated by the values for the molecular hydrogen ion. Assuming R-independent corrections, the radiative correction of the H(1s) + H(2l) dissociation threshold is only 12.5% larger than the value of the H(1s) + H$^+$ threshold, because of the n^{-3} proportionality of the leading-order term of the radiative correction. The difference of the leading-order radiative corrections for the X$^+$(0,0) and X(0,0) states is ~ -0.4 cm^{-1}. Consequently a shift of ~ -1.3 cm^{-1} ($= -0.9$ cm$^{-1} - 0.4$ cm^{-1}) might be expected, which would reduce the discrepancy to less than -0.3 cm^{-1} for the H($v = 1$, $N = 0$) and less than -2 cm^{-1} for the GK($v = 0$–2, $N = 0$) levels. We attribute these residual negative deviations to the effects of nonadiabatic couplings to higher-lying singlet gerade states not included in the close-coupling calculations. This is supported by the strong N dependence, which points to an underestimated or neglected heterogeneous coupling. Including higher electronic states in the close-coupling calculations of nonadiabatic corrections would severely complicate them. The problem of the explicit treatment of the coupled electronic states could be circumvented by using pre-Born–Oppenheimer techniques[10,11,14] or a multichannel quantum-defect approach.[35]

4.2 Lifetimes

The measured lifetimes (see Table 2) depend on the electronic, vibrational and rotational states. They are plotted in Fig. 6(d) as a function of N relative to the lifetime of the $N = 0$ level of the respective vibronic state. The N dependence of the lifetimes does not correlate with the strength of the nonadiabatic coupling. This observation corroborates the conclusions of earlier works (see ref. 19) that the dominant decay process for these states is of radiative nature. The only accessible dissociation continuum, associated with the H(1s) + H(1s) dissociation threshold, is related to the X $^1\Sigma_g^+$ state. The large continuum energy results in rapidly oscillating nuclear wavefunctions with vanishing overlaps with the GK and H nuclear wavefunctions. For the GK state, the lifetimes are correlated to the wavefunction amplitudes in the inner and outer wells (see inset of Fig. 1), the inner well levels decaying faster. The observed behaviour can be attributed to a smaller overlap of the nuclear wave function of the GK($v = 0$, 2) states with the B $^1\Sigma_u^+$ and C $^1\Pi_u$ states and the increasing ($1s\sigma_g 2s\sigma_g$) character (*i.e.*, the character of the inner well of the EF state) of the GK state at larger internuclear distances. The longest lifetimes are those of the H($v = 0$) level and the shortest are those of the I$^+$ and GK($v = 1$) levels.

In the previous section, a systematic discrepancy was noted between the lifetimes measured in the present work and the lifetimes reported in the survey of Astashkevich and Lavrov,[20] the lifetimes obtained in the present work being shorter in almost all cases. The experimental lifetimes of the GK and H states in ref. 20 originate primarily from the measurements reported in ref. 32–34. Day *et al.*[32] and Sanchez *et al.*[34] both used electron impact excitation to excite different rovibrational levels of the $^1\Sigma_g^+$ states in gas cells and measured the decay of the fluorescence signal. Day *et al.*[32] observed pressure-dependent lifetimes and performed zero-pressure extrapolation, whereas Sanchez *et al.*[34] did not observe any pressure dependence. In both investigations, the lifetimes measured for many vibrational levels were found to be independent of the rotational quantum number. Tsukiyama *et al.*[33] used ultraviolet-visible double-resonance excitation to excite the $^1\Sigma_g^+$ states in a molecular beam and measured fluorescence lifetimes by imaging the fluorescence emission onto a photomultiplier. In contrast to ref. 32 and 34, they observed a strong N-dependence of the lifetimes for all GK and H vibrational levels. Our lifetimes were derived from pump–probe experiments with background-free field-ionisation detection. The observed decays were found to be well described by single-exponential functions and were independently validated by the analysis of the linewidths determined in high-precision measurements of transitions to long-lived high Rydberg states. Our results agree qualitatively with the results of Tsukiyama *et al.*[33] but differ in the quantitative aspects.

On the theoretical side, Quadrelli and Dressler[15] calculated the lifetimes of the rovibrational levels taking into account both spontaneous emission and predissociation. They suggested that the partial disagreement with older experimental data might arise from nonadiabatic effects not included in their treatment. Tsukiyama *et al.*[33] performed lifetime calculations based on the transition moments reported by Dressler and coworkers.[36] A good agreement between experimental and theoretical lifetimes was only found for the I$^+$($v = 0$) state. For the H state, Astashkevich and Lavrov[20] list the theoretical values obtained by Ross and coworkers[37] and seem to have overlooked that these values are for the outer-well state $\bar{\text{H}}$. Consequently, we list the values obtained by Yu and Dressler[29] for H($v = 0$, $N = 0$, 1), which are the only theoretical lifetimes in Table 2 that are shorter than our experimental results.

5 Conclusions

The properties of the ground electronic state of molecular hydrogen can be determined with remarkable accuracy in calculations that include nonadiabatic interactions and relativistic and radiative corrections.[2,3,13,14] Calculations of the properties of electronically excited states of molecular hydrogen do not reach, by far, the same degree of accuracy because of the increased complexity stemming from the increased level density.

We have determined the term values of several rovibrational levels of the GK and H $^1\Sigma_g^+$ states of H_2 with absolute and relative accuracies of 10^{-4} cm^{-1} and 10^{-6} cm^{-1}, respectively, in precision spectroscopic measurements carried out with skimmed supersonic beams and continuous-wave single-mode near-infrared laser radiation. Available theoretical term values deviate from our experimental values, the differences originating from the incomplete treatment of nonadiabatic, relativistic and radiative corrections.

 This journal is © the Owner Societies 2018

The comparison points at a need for the development of improved theoretical methods to calculate electronically excited states. Our experimental results represent a data set to test the accuracy of such calculations.

We have also determined the lifetimes of rovibrational levels of the GK, H and I^+ states of H_2 and found significant discrepancies with both earlier experimental and theoretical results. Our results contribute to filling gaps in the current knowledge of the dynamics of electronically excited states of H_2 and also point at a need for improved calculations of the properties of the excited states.

Conflicts of interest

There are no conflicts to declare.

Acknowledgements

The authors thank J. A. Agner and H. Schmutz (ETH Zürich) for their contributions to the development of the experimental apparatus. They also thank Prof. Ch. Jungen (Orsay), Prof. K. Dressler (Zürich), Prof. B. Jeziorski (Warsaw) and Prof. L. Wolniewicz (Torun) for stimulating discussions concerning the excited states of H_2. This work was supported by the Swiss National Science Foundation (Project No. 200020-172620) and by the European Research Council (ERC-Advanced Grant No. 743121).

Notes and references

1 V. I. Korobov, L. Hilico and J.-P. Karr, *Phys. Rev. Lett.*, 2017, **118**, 233001.
2 M. Puchalski, J. Komasa and K. Pachucki, *Phys. Rev. A*, 2017, **95**, 052506.
3 L. M. Wang and Z.-C. Yan, *Phys. Rev. A*, 2018, **97**, 060501.
4 J. Biesheuvel, J.-P. Karr, L. Hilico, K. Eikema, W. Ubachs and J. Koelemeij, *Nat. Commun.*, 2016, **7**, 10385.
5 C.-F. Cheng, J. Hussels, M. Niu, H. L. Bethlem, K. S. E. Eikema, E. J. Salumbides, W. Ubachs, M. Beyer, N. Hölsch, J. A. Agner, F. Merkt, L.-G. Tao, S.-M. Hu and C. Jungen, *Phys. Rev. Lett.*, 2018, **121**, 013001.
6 K. Pachucki and J. Komasa, *Phys. Rev. A: At., Mol., Opt. Phys.*, 2011, **83**, 042510.
7 M. Beyer and F. Merkt, to be published.
8 K. Pachucki and J. Komasa, *J. Chem. Phys.*, 2008, **129**, 034102.
9 K. Pachucki and J. Komasa, *J. Chem. Phys.*, 2009, **130**, 164113.
10 W. Kołos and L. Wolniewicz, *Rev. Mod. Phys.*, 1963, **35**, 473–483.
11 E. Mátyus and M. Reiher, *J. Chem. Phys.*, 2012, **137**, 024104.
12 K. Pachucki and J. Komasa, *Phys. Chem. Chem. Phys.*, 2018, **20**, 247–255.
13 J. Komasa, K. Piszczatowski, G. Łach, M. Przybytek, B. Jeziorski and K. Pachucki, *J. Chem. Theory Comput.*, 2011, **7**, 3105–3115.
14 M. Puchalski, A. Spyszkiewicz, J. Komasa and K. Pachucki, *Phys. Rev. Lett.*, 2018, **121**, 073001.
15 P. Quadrelli, K. Dressler and L. Wolniewicz, *J. Chem. Phys.*, 1990, **92**, 7461–7478.
16 L. Wolniewicz, *J. Chem. Phys.*, 1998, **109**, 2254–2256.
17 R. K. Altmann, L. S. Dreissen, E. J. Salumbides, W. Ubachs and K. S. E. Eikema, *Phys. Rev. Lett.*, 2018, **120**, 043204.
18 M. Beyer, N. Hölsch, J. A. Agner, J. Deiglmayr, H. Schmutz and F. Merkt, *Phys. Rev. A*, 2018, **97**, 012501.
19 P. Quadrelli, K. Dressler and L. Wolniewicz, *J. Chem. Phys.*, 1990, **93**, 4958–4964.
20 S. Astashkevich and B. Lavrov, *J. Phys. Chem. Ref. Data*, 2015, **44**, 023105.
21 L. Wolniewicz, http://fizyka.umk.pl/publications/ifiz/luwo/Index.
22 D. Jennings, S. Bragg and J. Brault, *Astrophys. J.*, 1984, **282**, L85–L88.
23 V. I. Korobov, *Phys. Rev. A: At., Mol., Opt. Phys.*, 2006, **73**, 024502.
24 V. I. Korobov, *Phys. Rev. A: At., Mol., Opt. Phys.*, 2006, **74**, 052506.
25 V. I. Korobov, *Phys. Rev. A: At., Mol., Opt. Phys.*, 2008, **77**, 022509.
26 H. Naus, I. H. van Stokkum, W. Hogervorst and W. Ubachs, *Appl. Opt.*, 2001, **40**, 4416–4426.
27 A. Osterwalder, A. Wüest, F. Merkt and Ch. Jungen, *J. Chem. Phys.*, 2004, **121**, 11810–11838.
28 D. Bailly, E. J. Salumbides, M. Vervloet and W. Ubachs, *Mol. Phys.*, 2010, **108**, 827–846.
29 S. Yu and K. Dressler, *J. Chem. Phys.*, 1994, **101**, 7692–7706.
30 M. Beyer, N. Hölsch, Ch. Jungen and F. Merkt, unpublished results.
31 D. Sprecher, M. Beyer and F. Merkt, *Mol. Phys.*, 2013, **111**, 2100–2107.
32 R. Day, R. Anderson and F. Sharpton, *J. Chem. Phys.*, 1979, **71**, 3683–3688.
33 K. Tsukiyama, J. Ishii and T. Kasuya, *J. Chem. Phys.*, 1992, **97**, 875–882.
34 J. A. Sanchez and J. Campos, *J. Phys.*, 1988, **49**, 445–449.
35 S. C. Ross and Ch. Jungen, *Phys. Rev. A: At., Mol., Opt. Phys.*, 1994, **50**, 4618–4628.
36 M. Glass-Maujean, P. Quadrelli and K. Dressler, *At. Data Nucl. Data Tables*, 1984, **30**, 273–300.
37 S. C. Ross, T. Yoshinari, Y. Ogi and K. Tsukiyama, *J. Chem. Phys.*, 2006, **125**, 133205.